

# Probing stops in the coannihilation region at the HL-LHC: a comparative study of different processes

Guang Hua Duan<sup>1,2</sup>, Xiang Fan<sup>1,2</sup>, Ken-ichi Hikasa<sup>3</sup>, Bo Peng<sup>1,2</sup>, and Jin Min Yang<sup>1,2,3</sup>

<sup>1</sup> *CAS Key Laboratory of Theoretical Physics, Institute of Theoretical Physics,  
Chinese Academy of Sciences, Beijing 100190, China*

<sup>2</sup> *School of Physical Sciences, University of Chinese  
Academy of Sciences, Beijing 100049, China*

<sup>3</sup> *Department of Physics, Tohoku University, Sendai 980-8578, Japan*

## Abstract

In the minimal supersymmetric model, the coannihilation of the lighter stop  $\tilde{t}_1$  and bino-like dark matter  $\chi$  provides a feasible way to accommodate the correct dark matter relic abundance. In this scenario, due to the compressed masses,  $\tilde{t}_1$  merely appears as missing energy at the LHC and thus the pair production of  $\tilde{t}_1$  can only be probed by requiring an associated energetic jet. Meanwhile, since  $\tilde{t}_2$  and  $\tilde{b}_1$  are correlated in mass and mixing with  $\tilde{t}_1$ , the production of  $\tilde{t}_2\tilde{t}_2^*$  or  $\tilde{b}_1\tilde{b}_1^*$ , each of which dominantly decays into  $\tilde{t}_1$  plus  $Z$ ,  $h$  or  $W$  boson, may serve as a complementary probe. We examine all these processes at the HL-LHC and find that the  $2\sigma$  sensitivity to  $\chi$  mass can be as large as about 570 GeV, 600 GeV and 1.1 TeV from the production process of  $\tilde{t}_1\tilde{t}_1^* + \text{jet}$ ,  $\tilde{t}_2\tilde{t}_2^*$  and  $\tilde{b}_1\tilde{b}_1^*$ , respectively.

## I. INTRODUCTION

The nature of dark matter (DM) remains a mystery in particle physics. In minimal supersymmetric standard model (MSSM) with conserved  $R$ -parity, the lightest neutralino  $\chi$  can serve as a DM candidate. However, the null results of DM direct detections [1–3] give significant constraints on the neutralino sector in the MSSM. It is notable that the stop-bino coannihilation, in which DM is the bino-like lightest supersymmetric particle (bino-LSP) and the stop ( $\tilde{t}_1$ ) is the next-to-lightest supersymmetric particle (NLSP) and nearly degenerate with the bino-LSP, provides a feasible mechanism to accommodate the DM relic abundance. Because of the extremely weak interaction between the bino-LSP and nucleons, this scenario can easily evade the DM direct detection constraints [4]. However, the search of stops at the LHC in this scenario is rather challenging<sup>1</sup>. The reason is that due to the compressed masses,  $\tilde{t}_1$  is merely appearing as missing energy and the pair production of  $\tilde{t}_1$  can only be probed by requiring an associated energetic jet.

On the other hand, we should note that  $\tilde{t}_2$  and  $\tilde{b}_1$  are correlated with  $\tilde{t}_1$  since  $\tilde{t}_{L,R}$  mix into mass eigenstates  $\tilde{t}_{1,2}$  (see the following section) while  $\tilde{b}_L$  ( $\tilde{b}_1 = \tilde{b}_L$ , neglecting the sbottom mixing) has the same soft mass as  $\tilde{t}_L$ . Furthermore, to avoid fine-tuning, these particles should not be too heavy<sup>2</sup> because at one-loop level we approximately have [13, 14]

$$\Delta \equiv \frac{\delta m_h^2}{m_h^2} = \frac{3y_t^2}{4\pi^2 m_h^2} (m_{Q_3}^2 + m_{U_3}^2 + A_t^2) \log \frac{\Lambda}{m_{\text{SUSY}}} \quad (1)$$

where  $m_{\text{SUSY}} = \sqrt{m_{\tilde{t}_1} m_{\tilde{t}_2}}$ ,  $\Lambda$  is the cut-off scale,  $Q_3 = (\tilde{t}_L, \tilde{b}_L)$  and  $U_3 = \tilde{t}_R$ . Therefore, the production of  $\tilde{t}_2 \tilde{t}_2^*$  or  $\tilde{b}_1 \tilde{b}_1^*$ , followed by the dominant decays into  $\tilde{t}_1$  plus  $Z$ ,  $h$  or  $W$  boson, may serve as a complementary probe of stops in such a stop-bino coannihilation scenario.

In this work we perform a comprehensive study for all these correlated processes at the HL-LHC (14 TeV, 3000 fb<sup>-1</sup>). We will first perform a scan to figure out the stop-bino coannihilation parameter space. Then we display the properties of  $\tilde{t}_{1,2}$  and  $\tilde{b}_1$  in this stop-bino coannihilation parameter space. For the  $\tilde{t}_1 \tilde{t}_1^* + \text{jet}$  production which has been searched at the LHC, we will show its current sensitivity and then extend the coverage to the HL-

<sup>1</sup> The search of stops at the LHC has been a hot topic and numerous studies have been performed in various cases, e.g., the large or small stop-top or stop-LSP mass splitting [5–7], the single stop production [8], the stop in natural SUSY [9], machine learning in stop production [10] and other miscellaneous cases [11].

<sup>2</sup> Note that the stops cannot be too light in order to give the 125 GeV Higgs mass except a singlet is introduced [12].

LHC. For the productions  $\tilde{t}_2\tilde{t}_2^*$  and  $\tilde{b}_1\tilde{b}_1^*$ , followed the dominant decays  $\tilde{t}_2 \rightarrow \tilde{t}_1 + Z/h$  and  $\tilde{b}_1 \rightarrow \tilde{t}_1 + W$ , we will examine the HL-LHC sensitivities through Monte Carlo simulations of the signals and backgrounds.

The structure of this paper is organized as follows. In Sec. II, we briefly review stop-bino coannihilation scenario and discuss the details of our scan. In Sec. III, we perform detailed Monte Carlo simulations for the productions of  $\tilde{t}_1\tilde{t}_1^* + \text{jet}$ ,  $\tilde{t}_2\tilde{t}_2^*$  and  $\tilde{b}_1\tilde{b}_1^*$  at the HL-LHC. Finally, we give our conclusions in Sec. IV.

## II. STOP-BINO COANNIHILATION

In the MSSM, the mass matrix of stop sector in gauge-eigenstate basis  $(\tilde{t}_L, \tilde{t}_R)$  is given by

$$M_{\tilde{t}}^2 = \begin{pmatrix} m_{\tilde{t}_L}^2 & m_t X_t^\dagger \\ m_t X_t & m_{\tilde{t}_R}^2 \end{pmatrix} \quad (2)$$

where

$$m_{\tilde{t}_L}^2 = m_{\tilde{Q}_{3L}}^2 + m_t^2 + m_Z^2 \left( \frac{1}{2} - \frac{2}{3} \sin^2 \theta_W \right) \cos 2\beta, \quad (3)$$

$$m_{\tilde{t}_R}^2 = m_{\tilde{U}_{3R}}^2 + m_t^2 + \frac{2}{3} m_Z^2 \sin^2 \theta_W \cos 2\beta, \quad (4)$$

$$X_t = A_t - \mu \cot \beta. \quad (5)$$

The mixing between  $\tilde{t}_L$  and  $\tilde{t}_R$  is induced by  $X_t = A_t - \mu \cot \beta$ , where  $A_t$  is the stop soft-breaking trilinear coupling. One can diagonalize the mass matrix through a rotation

$$\begin{pmatrix} \tilde{t}_1 \\ \tilde{t}_2 \end{pmatrix} = \begin{pmatrix} \cos \theta_{\tilde{t}} & \sin \theta_{\tilde{t}} \\ -\sin \theta_{\tilde{t}} & \cos \theta_{\tilde{t}} \end{pmatrix} \begin{pmatrix} \tilde{t}_L \\ \tilde{t}_R \end{pmatrix}, \quad (6)$$

where  $\tilde{t}_1$  and  $\tilde{t}_2$  are the mass eigenstates of lighter and heavier stops, respectively. The mixing angle  $\theta_{\tilde{t}}$  between  $\tilde{t}_L$  and  $\tilde{t}_R$  is determined by

$$\tan 2\theta_{\tilde{t}} = \frac{2m_t X_t}{m_{\tilde{t}_L}^2 - m_{\tilde{t}_R}^2}. \quad (7)$$

In the early universe, the freeze-out number density for the bino-LSP DM will be overabundant because the annihilation cross section  $\sigma$  in the Boltzmann equation is too small to keep DM thermal equilibrium with SM particles for sufficient time<sup>3</sup>. When the stop ( $\tilde{t}_1$ )

<sup>3</sup> The  $Z/h$  funnel as another exception is that the annihilation cross section could be enhanced when bino-LSP mass becomes half of  $m_{Z/h}$ .

mass is close to bino-LSP mass, the annihilation cross section  $\sigma$  is replaced by the effective cross section [15]

$$\sigma_{\text{eff}} = \sum_{ij} \sigma_{ij} r_i r_j \quad (8)$$

with

$$r_i = \frac{g_i (1 + \Delta_i)^{3/2} e^{-\Delta_i/T}}{\sum_k g_k (1 + \Delta_k)^{3/2} e^{-\Delta_k/T}} \quad (9)$$

where  $\Delta_i = (m_i - m_\chi)/T$ ,  $m_i$  and  $g_i$  are the mass and degrees of freedom of the particle  $i = \{\chi, \tilde{t}_1\}$ , and  $\sigma_{ij}$  denotes the cross section of particle  $i$  annihilating with particle  $j$ . The annihilation modes of  $\tilde{t}_1$  with  $\chi$  or itself can enhance  $\sigma_{\text{eff}}$  if  $\tilde{t}_1$  is nearly degenerate with the bino-LSP. We can also see that  $\sigma_{\tilde{t}_1 \tilde{t}_1}$  is suppressed by double exponents compared to  $\sigma_{\chi\chi}$ , while  $\sigma_{\tilde{t}_1 \chi}$  is suppressed by single exponent. Therefore, when the mass splitting  $\Delta_{\tilde{t}_1}$  is small, the contribution to relic abundance from the  $\tilde{t}_1 \chi$  annihilation tends to be more important than that from the  $\tilde{t}_1 \tilde{t}_1^*$  annihilation, although this also depends on their respective cross section.

In order to obtain the stop-bino coannihilation parameter space, we use **SuSpect 2.41** [16] to calculate the mass spectrum and **SDECAY 1.5** [17] to evaluate sparticle decay width and branching ratio. We regard the lighter stop as right-handed dominated. The reason for such assumption is that if  $m_{\tilde{t}_R} = m_{\tilde{t}_L}$  at some high energy scale,  $m_{\tilde{t}_R}$  tends to be smaller than  $m_{\tilde{t}_L}$  at the electroweak scale from the renormalization group equations (RGE) evolution [18]. The stop mixing angle  $\cos^2 \theta_{\tilde{t}} \lesssim 0.5$  is required so that the lighter stop  $\tilde{t}_1$  is right-handed dominant. Except for  $\{M_1, m_{Q_3}, m_{U_3}, A_t\}$ , other soft-breaking masses (including the CP-odd Higgs mass  $M_A$ ) and trilinear couplings are set to 5 TeV and zero, respectively. The higgsino mass parameter  $\mu$  and  $\tan \beta$  are chosen as 3 TeV and 20. The **micrOMEGAs 4.3.5** [19] is used to compute the DM relic abundance  $\Omega_\chi h^2$ .

In our scan we impose the following constraints<sup>4</sup>:

- (i) The lighter CP-even Higgs mass is required to be in the range of  $125 \pm 3$  GeV [20, 22].
- (ii) The DM relic abundance satisfies the observed value  $\Omega_\chi h^2 = 0.1186 \pm 0.0020$  within  $2\sigma$  range [23].

---

<sup>4</sup> Here we do not require SUSY to explain the muon g-2 anomaly, which requires light sleptons [21]

- (iii) To avoid the existence of a color or charge breaking vacuum deeper than the electroweak vacuum in the scalar potential, the trilinear coupling  $A_t$  should not exceed the upper bound  $A_t^2 \lesssim 2.67(m_{\tilde{t}_L}^2 + m_{\tilde{t}_R}^2 + \mu^2 + m_{H_u}^2)$  [24].

In the left panel of Fig. 1, we display the stop-bino coannihilation parameter space that satisfies the constraints (i)–(iii), where the  $B$  physics constraints are ignored because of the decoupled higgsino mass parameter, and the contribution of the stops to  $h \rightarrow \gamma\gamma$  (and  $gg$ ) [18] is also negligibly small. We can see that the mass splitting  $\Delta m(\tilde{t}_1, \chi)$  increases with  $|\cos\theta_{\tilde{t}}|$  because the component of left-handed stop annihilates with itself more efficiently due to the  $SU(2)_L$  interaction. Besides, it can be seen that the maximal value of  $m_\chi$  is about 1.8 TeV, where  $\tilde{t}_1\tilde{t}_1^* \rightarrow gg$  is the dominant annihilation mode because of the QCD interaction and small mass splitting  $\Delta m(\tilde{t}_1, \chi)$  or small  $\Delta_{\tilde{t}_1}$ .

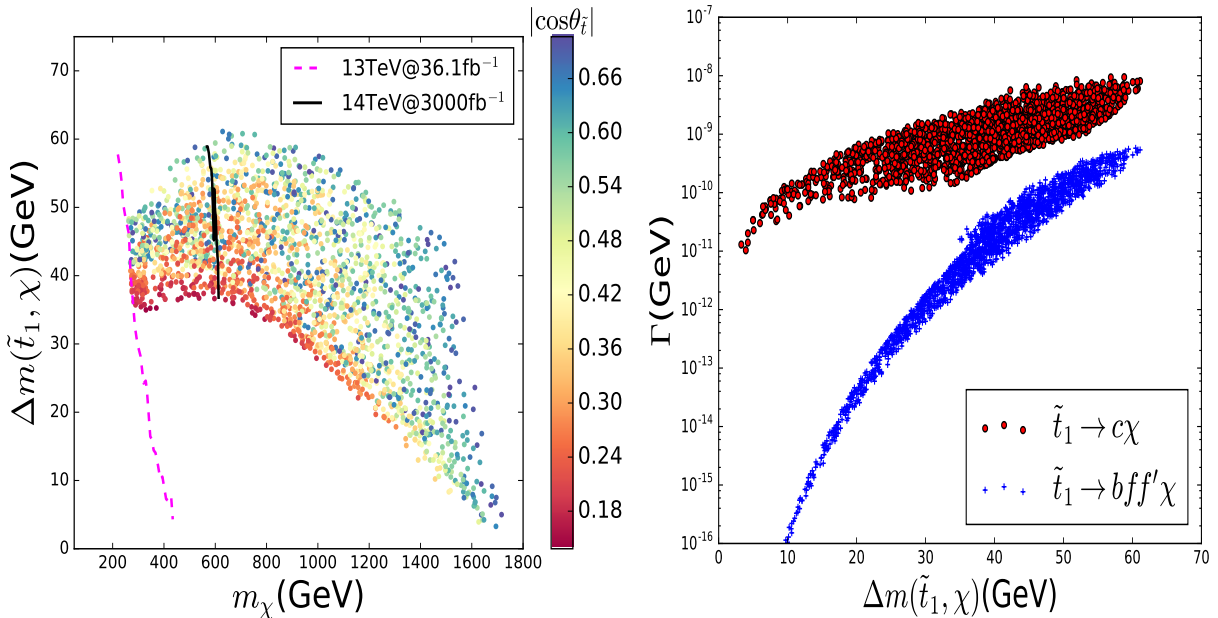


FIG. 1: Scatter plots of the stop-bino coannihilation parameter space satisfying the constraints (i)–(iii). The left panel shows the DM mass  $m_\chi$  versus mass splitting  $\Delta m(\tilde{t}_1, \chi)$  with the colormap denoting the size of  $|\cos\theta_{\tilde{t}}|$ . The dashed magenta curve and the solid black curve are the  $2\sigma$  sensitivities of the  $\tilde{t}_1\tilde{t}_1^* + \text{jet}$  production from the current ATLAS search [25] and our simulations for the HL-LHC, respectively. The right panel shows the stop  $\tilde{t}_1$  decay width of the four-body channel  $\tilde{t}_1 \rightarrow b f \bar{f}' \chi$  and the FCNC two-body channel  $\tilde{t}_1 \rightarrow c \chi$ .

### III. PROBING STOPS IN THE COANNIHILATION REGION AT THE HL-LHC

#### A. The $\tilde{t}_1\tilde{t}_1^* + \text{jet}$ production

Since the lighter stop is nearly degenerate with the bino-LSP, the two-body decay channel  $\tilde{t}_1 \rightarrow t\chi$  and three-body decay channel  $\tilde{t}_1 \rightarrow bW\chi$  are kinematically forbidden. The lighter stop will dominantly decay via the four-body channel  $\tilde{t}_1 \rightarrow bf\bar{f}'\chi$  and loop induced flavor-changing neutral current (FCNC) two-body channel  $\tilde{t}_1 \rightarrow c\chi$ . The contribution to  $\tilde{t}_1 \rightarrow bf\bar{f}'\chi$  comes from the top quark exchange diagram and the interference between top quark and sfermions exchange diagrams because sparticles, except for  $\tilde{t}_{1,2}, \tilde{b}_1$  and  $\chi$ , are decoupled in our scenario. The flavor mixing of the lighter stop with charm-squark which can emerge from radiative corrections induces the lighter stop FCNC decay  $\tilde{t}_1 \rightarrow c\chi$ . Their decay widths are given by [26–29]

$$\Gamma(\tilde{t}_1 \rightarrow c\chi) = \frac{8}{9}\alpha|\epsilon|^2 \frac{\Delta m(\tilde{t}_1, \chi)^2}{m_{\tilde{t}_1}}, \quad (10)$$

$$\Gamma_{4\text{-body}} \equiv \Gamma(\tilde{t}_1 \rightarrow bf\bar{f}'\chi) = \mathcal{O}(10^{-5}) \alpha^3 \cos^2 \theta_t \frac{\Delta m(\tilde{t}_1, \chi)^8}{m_t^2 m_W^4 m_{\tilde{t}_1}}, \quad (11)$$

where  $\epsilon$  is  $\mathcal{O}(10^{-4})$  if all soft-breaking parameters have the same order of magnitude. It is clear that the four-body decay width increases more sharply with  $\Delta m(\tilde{t}_1, \chi)$  than the FCNC two-body decay width, as shown in the right panel of Fig. 1. However, due to the ratio of  $\Gamma_{4\text{-body}}/\Gamma(\tilde{t}_1 \rightarrow c\chi)$  is suppressed by  $\Delta m(\tilde{t}_1, \chi)^6/m_t^2 m_W^4$  and the small coefficient, the four-body decay is not competitive with the  $\tilde{t}_1 \rightarrow c\chi$  decay.

Because the soft  $c$ -jet from the  $\tilde{t}_1 \rightarrow c\chi$  decay is hard to detect, the search strategy for this coannihilation scenario is usually to exploit the  $\tilde{t}_1\tilde{t}_1^*$  production in association with an energetic jet from the initial state radiation (ISR) which boosts  $\tilde{t}_1\tilde{t}_1^*$  system and produces large missing energy at the LHC. The parton level events of the signal and backgrounds are generated with `MadGraph5_aMC@NLO` [30]. Then, the event parton showering and hadronization are performed by `Pythia` [31]. We use `Delphes` [32] to implement detector simulations where the anti- $k_t$  jet algorithm and  $\Delta R = 0.4$  [33] are set for the jet clustering.

To discriminate the signal and backgrounds, we require a leading jet with  $p_T(j_1) > 300$  GeV,  $|\eta| < 2.4$  and azimuthal angle  $\Delta\phi(j_1, \vec{p}_T^{\text{miss}}) > 0.4$ . We veto events with electrons with  $p_T > 20$  GeV,  $|\eta| < 2.47$  or muons with  $p_T > 10$  GeV,  $|\eta| < 2.5$  to reduce the  $W(\rightarrow \ell\nu_\ell)j$  and  $t\bar{t}$  backgrounds. Events having more than four jets with  $p_T > 30$  and  $|\eta| < 2.8$  are

vetoed. The signal regions are defined with  $E_T^{\text{miss}}$  cuts: 300 GeV, 500 GeV, 700 GeV and 900 GeV. The signal significance is calculated as  $S/\sqrt{B}$  in which the total background  $B = \sum_i [B_i + (0.01B_i)^2]$  ( $i = Z(\rightarrow \nu\bar{\nu})j, W(\rightarrow \ell\nu_\ell)j, W(\rightarrow \tau\nu_\tau)j$ ), where the systematic error on the backgrounds is set to 1%.

In the left panel of Fig. 1, we display the  $2\sigma$  exclusion limits at the 13 TeV LHC with  $\mathcal{L} = 36.1 \text{ fb}^{-1}$  (the region on the left side of the curve is excluded) and the sensitivity at the 14 TeV LHC with  $\mathcal{L} = 3000 \text{ fb}^{-1}$ . We can see that the current monojet search gives a loose limit on the bino-LSP DM mass  $m_\chi \gtrsim 260 \text{ GeV}$  and this limit can be raised to 570 GeV at the 14 TeV LHC with  $\mathcal{L} = 3000 \text{ fb}^{-1}$ .

## B. The $\tilde{t}_2\tilde{t}_2^*$ production

From the naturalness argument in Sec. I,  $\tilde{t}_2$  can not be too heavy and the  $\tilde{t}_2\tilde{t}_2^*$  production can be sizable at the LHC. Since the LSP is bino-like in our scenario, the  $\tilde{t}_2$  decay modes are mainly  $\tilde{t}_2 \rightarrow \tilde{t}_1 Z$  and  $\tilde{t}_2 \rightarrow \tilde{t}_1 h$ . The corresponding decay widths are given by [34]

$$\Gamma(\tilde{t}_2 \rightarrow \tilde{t}_1 Z) \approx \frac{g_2^2 \sin^2 2\theta_{\tilde{t}} m_{\tilde{t}_2}^3}{256\pi m_W^2} \lambda^{3/2}(m_{\tilde{t}_2}^2, m_{\tilde{t}_1}^2, m_Z^2), \quad (12)$$

$$\Gamma(\tilde{t}_2 \rightarrow \tilde{t}_1 h) \approx \frac{g_2^2 \cos^2 2\theta_{\tilde{t}} m_{\tilde{t}}^2 X_t^2}{64\pi m_W^2 m_{\tilde{t}_2}} \lambda^{1/2}(m_{\tilde{t}_2}^2, m_{\tilde{t}_1}^2, m_h^2), \quad (13)$$

where  $\lambda(a, b, c) = [1 - (b+c)/a]^2 - 4bc/a^2$  is the kinematic factor. In the limits  $m_{\tilde{t}_2}^2, m_{\tilde{t}_1}^2 \gg m_{Z,h}^2$ , the factor  $\lambda(m_{\tilde{t}_2}^2, m_{\tilde{t}_1}^2, m_{Z,h}^2)$  approximately equals to  $(1 - m_{\tilde{t}_1}^2/m_{\tilde{t}_2}^2)^2$  and then

$$\frac{\Gamma(\tilde{t}_2 \rightarrow \tilde{t}_1 h)}{\Gamma(\tilde{t}_2 \rightarrow \tilde{t}_1 Z)} \approx \cos^2 2\theta_{\tilde{t}} = 1 - \frac{4m_{\tilde{t}}^2 X_t^2}{(m_{\tilde{t}_2}^2 - m_{\tilde{t}_1}^2)^2}. \quad (14)$$

It should be noted that the decay width  $\Gamma(\tilde{t}_2 \rightarrow \tilde{t}_1 Z)$  is always larger than  $\Gamma(\tilde{t}_2 \rightarrow \tilde{t}_1 h)$  even though the small loop corrections are taken into account [35, 36]. In Fig.2, we plot the branching ratio of  $\tilde{t}_2 \rightarrow \tilde{t}_1 Z$  and  $\tilde{t}_2 \rightarrow \tilde{t}_1 h$ . It is clear that  $\text{Br}(\tilde{t}_2 \rightarrow \tilde{t}_1 h)$  is lower than  $\text{Br}(\tilde{t}_2 \rightarrow \tilde{t}_1 Z)$  and their difference decreases with the mass splitting  $\Delta m(\tilde{t}_2, \tilde{t}_1)$  between heavier and lighter stops. Since the masses of  $\tilde{t}_1$  and the bino-LSP are nearly degenerate, the  $\tilde{t}_1$  will appear as missing energy and the signal of  $\tilde{t}_2\tilde{t}_2^*$  production at the LHC is

$$pp \rightarrow \tilde{t}_2\tilde{t}_2^* \rightarrow ZZ + E_T^{\text{miss}} \quad \text{or} \quad Zh + E_T^{\text{miss}} \quad (15)$$

where we neglect the  $hh + E_T^{\text{miss}}$  channel because its production rate is smaller than the above channels. Here we investigate the  $2\ell 2b$  final states, in which leptons come from  $Z$  decay and

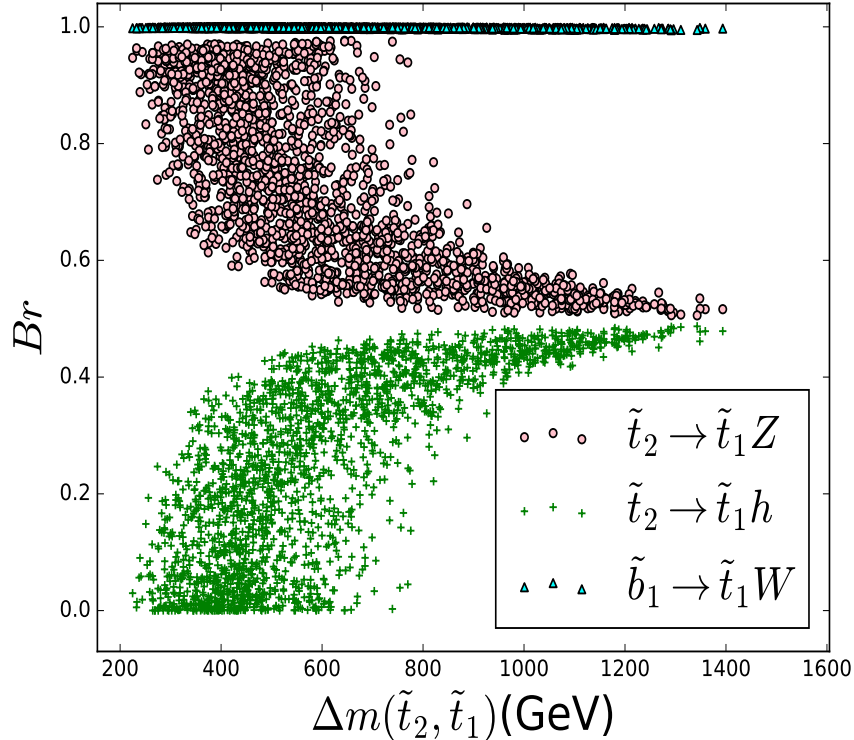


FIG. 2: Same as Fig.1, but showing the branching ratios of  $\tilde{t}_2 \rightarrow \tilde{t}_1 Z$ ,  $\tilde{t}_2 \rightarrow \tilde{t}_1 h$  and  $\tilde{b}_1 \rightarrow \tilde{t}_1 W$ .

bottom quarks are from  $Z/h$  decay, along with large missing energy. The requirement of two leptons can efficiently reduce the QCD multi-jets backgrounds<sup>5</sup>.

The main SM backgrounds are  $t\bar{t} + \text{jets}$ ,  $tWj$ ,  $ZZjj$  and  $WWjj$ . To discriminate the signal and backgrounds, the following cuts are imposed:

- (i) The event is required to have exact two leptons which form the opposite sign and same flavor dilepton with  $p_T(\ell) > 30$  GeV and  $|\eta_\ell| < 2.5$ , where  $\ell = e, \mu$ . According to the left panel of Fig. 3, the invariant masses of dilepton should be required in range of  $80 \text{ GeV} < m_{\ell\ell} < 100 \text{ GeV}$  to reconstruct  $Z$  bosons.
- (ii) Jets must have  $p_T(j) > 30$  GeV and  $|\eta_j| < 2.5$ . We require two  $b$ -jets and the  $b$ -jet tagging efficiency is set to be 80%.
- (iii) From the right panel of Fig. 3, the signal regions are designed according to  $E_T^{\text{miss}}$  cuts: 300 GeV, 350 GeV, 400 GeV, 450 GeV and 500 GeV.

<sup>5</sup> Tagging a soft  $c$ -jet from  $\tilde{t}_1$  [37] or boosted bosons  $Z/h$  [38] may help to suppress the backgrounds.



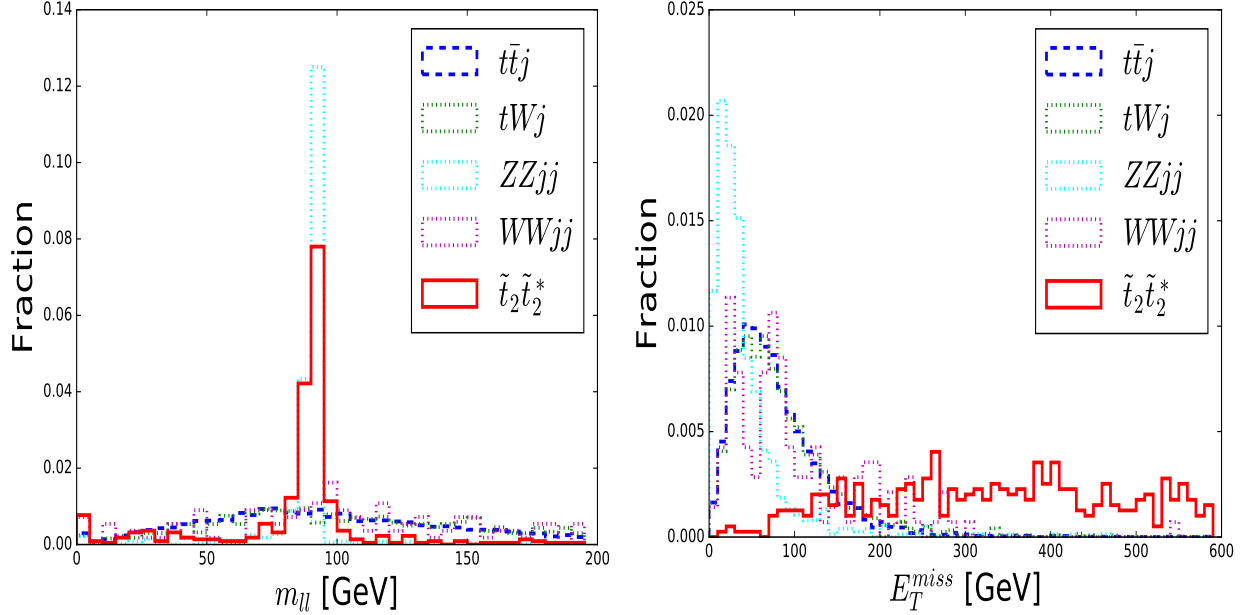


FIG. 3: The distributions of  $m_{\ell\ell}$  and  $E_T^{\text{miss}}$  for backgrounds and signal at the 14 TeV LHC after requiring exactly 2 leptons and 2  $b$ -jets. The signal benchmark point is chosen as  $(m_{\tilde{t}_2}, m_{\tilde{t}_1}, m_\chi) = (962, 468, 424)$  GeV.

TABLE I: The cut flow of events number for backgrounds and the signal at the HL-LHC. The signal benchmark point is  $(m_{\tilde{t}_2}, m_{\tilde{t}_1}, m_\chi) = (962, 468, 424)$  GeV.

cut	2 leptons $p_T^\ell > 30$ GeV, $ \eta^\ell  < 2.5$	2 $b$ -jets $p_T^b > 30$ GeV, $ \eta^b  < 2.5$	$ m_{\ell\ell} - m_Z  < 10$ [GeV]	$\cancel{E}_T > 450$ [GeV]
$t\bar{t}j$	1.248E+8	4.105E+7	5.849E+6	653
$tWj$	7.393E+6	1.349E+6	1.769E+5	30
$ZZjj$	7.212E+5	5.159E+4	4.531E+4	62
$WWjj$	2.603E+6	8.913E+4	1.506E+4	38
signal	3247	581	379	149

In Table I, a detailed cut flow of events number for backgrounds and the signal is displayed. We can see that the  $t\bar{t}j$  production is the largest SM background and the sum of other backgrounds is also non-negligible. The requirement of the two-lepton invariant mass within the range of 80–100 GeV can reduce the backgrounds by around 85%. It is clear that the cut of  $\cancel{E}_T > 450$  GeV can remove backgrounds by near four orders of magnitude and this is consistent with the distributions of the missing energy for backgrounds and the signal

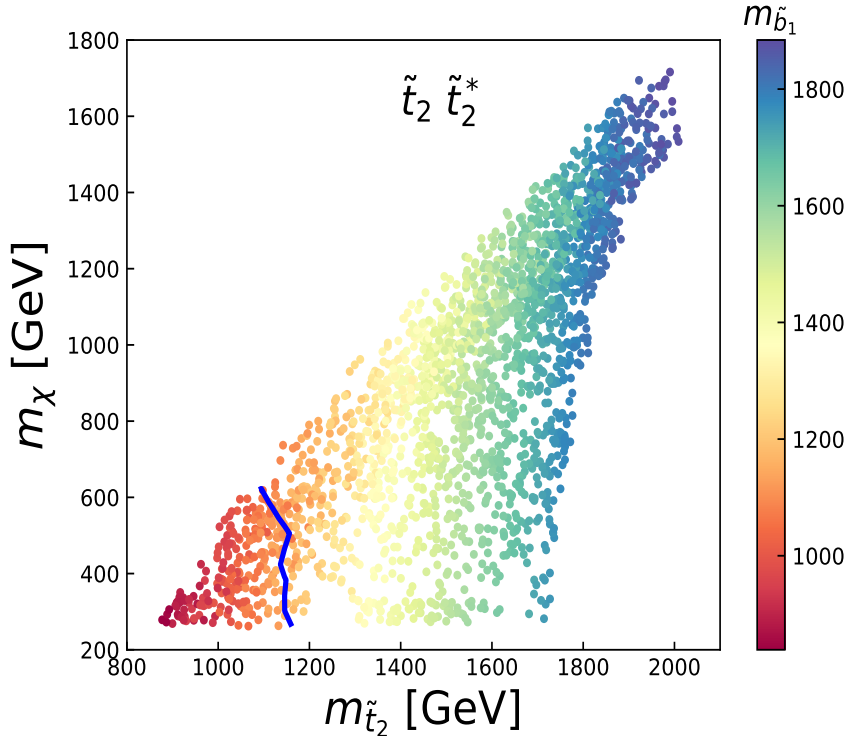


FIG. 4: Same as Fig. 1, but showing the observability of the  $\tilde{t}_2\tilde{t}_2^*$  production on the  $(m_{\tilde{t}_2}, m_\chi)$  plane. The colormap represents the lighter sbottom mass  $m_{\tilde{b}_1}$ . The blue curve is the  $2\sigma$  significance and the left region has a sensitivity above  $2\sigma$  level.

shown in Fig. 3. After imposing all these cuts, the significance  $S/\sqrt{B}$  for the benchmark point is about  $5.32\sigma$ .

In Fig. 4 we present the observability for the  $\tilde{t}_2\tilde{t}_2^*$  production. The points to the left of the blue curve have a sensitivity above  $2\sigma$  level and the colormap shows the change in  $m_{\tilde{b}_1}$ . We can see that this stop pair production can cover  $m_\chi \lesssim 600$  GeV for  $m_{\tilde{t}_2} \lesssim 1100$  GeV at  $2\sigma$  level. This result is not sensitive to the mass splitting  $\Delta m(\tilde{t}_1, \chi)$ .

### C. The $\tilde{b}_1\tilde{b}_1^*$ production

The sbottom  $\tilde{b}_1$  is lighter than the stop  $\tilde{t}_2$  because of the mixing between left and right handed stops. Since  $\tilde{b}_1$  is left-handed in our scenario, it could decay to the longitudinal component of  $W$  boson in association with  $\tilde{t}_1$ . The branching ratio of  $\tilde{b}_1 \rightarrow \tilde{t}_1 W$  is depicted in Fig. 2. As we see,  $\tilde{b}_1$  dominantly decays to  $W$  boson plus  $\tilde{t}_1$ . Then, the signal of  $\tilde{b}_1\tilde{b}_1^*$

production at the LHC is

$$pp \rightarrow \tilde{b}_1 \tilde{b}_1^* \rightarrow W^+ W^- + E_T^{\text{miss}}. \quad (16)$$

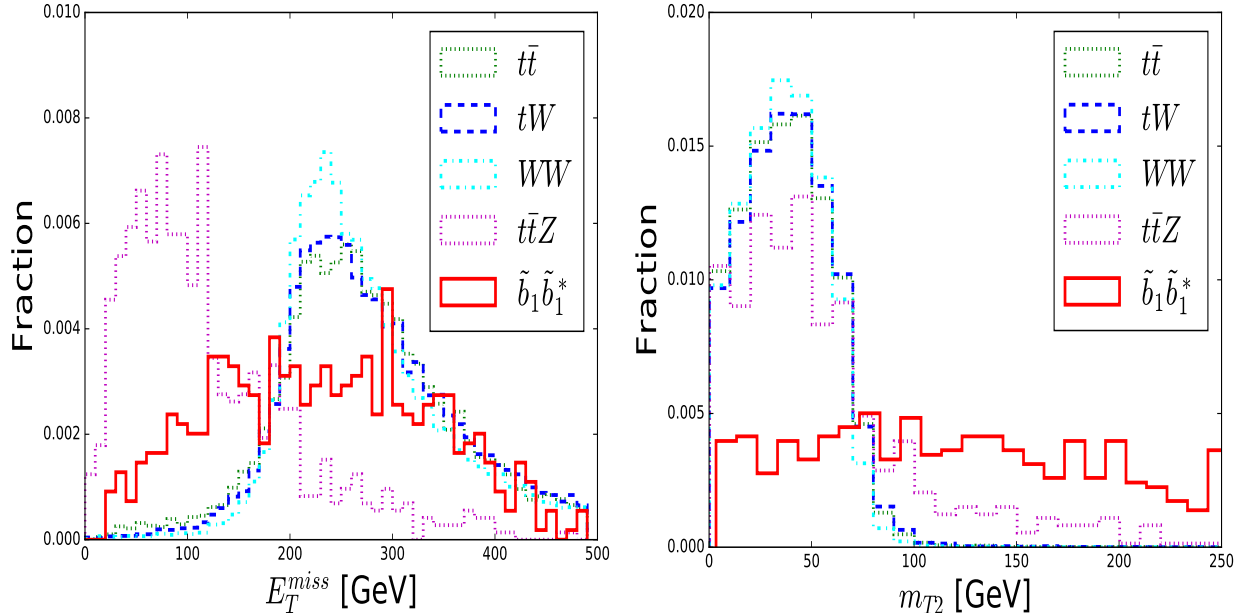


FIG. 5: The distributions of  $E_T^{\text{miss}}$  and  $m_{T2}$  for backgrounds and the signal at the 14 TeV LHC. The signal benchmark point is chosen as  $(m_{\tilde{b}_1}, m_{\tilde{t}_1}, m_\chi) = (1200, 910, 870)$  GeV.

TABLE II: The cut flow analysis of events number for backgrounds and the signal at the HL-LHC. The signal benchmark point is  $(m_{\tilde{b}_1}, m_{\tilde{t}_1}, m_\chi) = (1200, 910, 870)$  GeV.

cut	$t\bar{t}$	$tW$	$WW$	$t\bar{t}Z$	signal
$\sum_\ell p_T^\ell > 200$ GeV	251	82	234	2312	169
$p_T^b > 50$ GeV veto	119	54	226	810	142
$E_T^{\text{miss}} > 200$ GeV	112	52	221	179	103

Similar to the search in case of  $\text{Br}(\tilde{b}_1 \rightarrow \tilde{t}_1 W) = 1$  [39], we investigate  $2\ell E_T^{\text{miss}}$  final state to probe this sbottom pair production. We require exactly two opposite-sign leptons with  $p_T(\ell) > 25$  GeV and  $|\eta_\ell| < 2.4$  to suppress the QCD multi-jet backgrounds. The invariant mass of dilepton is required out of the range  $|m_{\ell\ell} - m_Z| < 30$  GeV to remove  $WZ$ ,  $ZZ$  and  $Z$ +jets backgrounds. Since the stop  $\tilde{t}_1$  boosts the  $W$  boson, the sum of the two leptons' transverse momentum  $\sum_\ell p_T^\ell > 200$  GeV can be used for further separating the

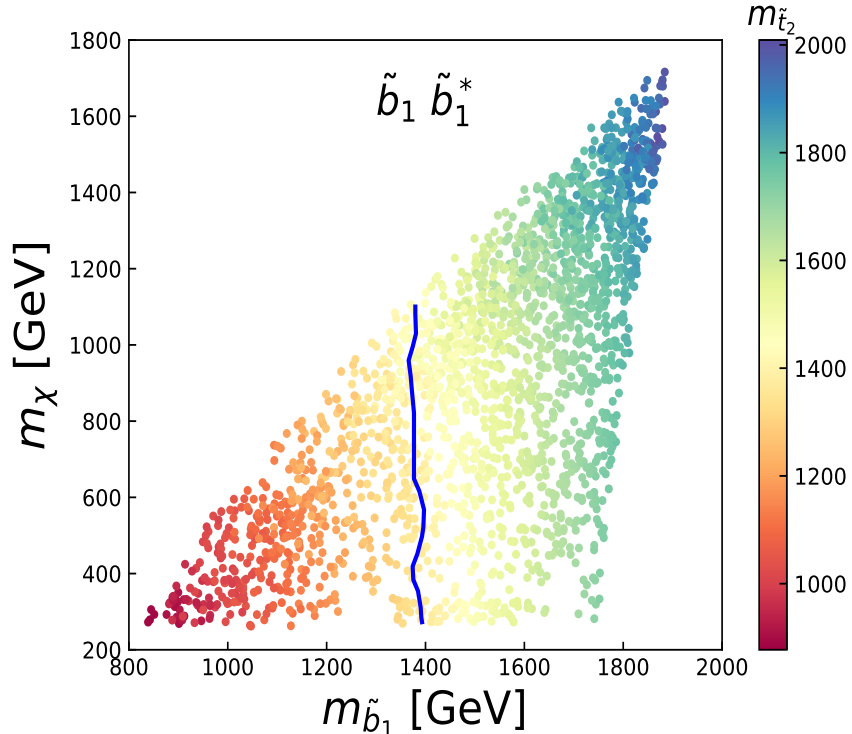


FIG. 6: Same as Fig. 1, but showing the observability of the  $\tilde{b}_1\tilde{b}_1^*$  production on the  $(m_{\tilde{b}_1}, m_\chi)$  plane. The colormap represents the change in  $m_{\tilde{t}_2}$ . The blue curve is the  $2\sigma$  significance and the left region has a sensitivity above  $2\sigma$  level.

signal from backgrounds. Any  $b$ -jet with  $p_T^b > 50$  GeV is vetoed for suppressing  $t\bar{t}$ ,  $tW$  and  $t\bar{t}Z$  backgrounds. A detailed cut flow of events number for backgrounds and the signal is displayed in Table II. After the  $\sum_\ell p_T^\ell > 200$  GeV requirement, we present the distributions of  $E_T^{\text{miss}}$  and  $m_{T2}$  of the two-lepton system in Fig. 5. It is clear that  $E_T^{\text{miss}} > 200$  GeV can reduce the  $t\bar{t}Z$  background efficiently. The variable  $m_{T2}$  of the backgrounds has an endpoint around  $M_W$ . For a larger  $m_{T2}$ , the  $t\bar{t}Z$  becomes the dominant background. We separate the signal regions according to  $m_{T2}$  cuts: 100 GeV, 150 GeV and 175 GeV.

We display the observability of the  $\tilde{b}_1\tilde{b}_1^*$  production in Fig. 6. It can be seen that such sbottom pair production can cover  $m_\chi \lesssim 1.1$  TeV for  $m_{\tilde{b}_1} \lesssim 1375$  GeV at  $2\sigma$  level. Correspondingly, the lower bound of  $m_{\tilde{t}_2}$  can be pushed up to around 1.4 TeV. Therefore, this result is obviously better than the  $\tilde{t}_2\tilde{t}_2^*$  production. This is mainly because this sbottom pair production has a cleaner signal.

## IV. CONCLUSIONS

We have studied the stop-bino coannihilation region, in which the observed dark matter relic abundance can be reproduced. To test the scenario, we have examined three correlated production processes  $\tilde{t}_1\tilde{t}_1^* + \text{jet}$  (the  $\tilde{t}_1$ 's being invisible),  $\tilde{t}_2\tilde{t}_2^*$  and  $\tilde{b}_1\tilde{b}_1^*$ , followed by the decays  $\tilde{t}_2 \rightarrow \tilde{t}_1 + Z/h$  and  $\tilde{b}_1 \rightarrow \tilde{t}_1 + W$ , at the HL-LHC. Through Monte Carlo simulations for the signals and backgrounds, we found that the  $2\sigma$  sensitivity to the bino-like LSP can reach about 570 GeV, 600 GeV and 1.1 TeV from the production process of  $\tilde{t}_1\tilde{t}_1^* + \text{jet}$ ,  $\tilde{t}_2\tilde{t}_2^*$  and  $\tilde{b}_1\tilde{b}_1^*$ , respectively. These three channels should be jointly considered at the future HL-LHC experiment.

## ACKNOWLEDGMENTS

We thank Lei Wu and Yang Zhang for helpful discussions. This work was supported by the National Natural Science Foundation of China (NNSFC) under grant Nos.11675242, 11821505, and 11851303, by Peng-Huan-Wu Theoretical Physics Innovation Center (11847612), by the CAS Center for Excellence in Particle Physics (CCEPP), by the CAS Key Research Program of Frontier Sciences and by a Key R&D Program of Ministry of Science and Technology under number 2017YFA0402204.

- 
- [1] X. Cui *et al.* (PandaX-II Collaboration), *Phys. Rev. Lett.* **119**, 181302 (2017) [arXiv:1708.06917 [astro-ph.CO]].
  - [2] E. Aprile *et al.* (XENON Collaboration), *Phys. Rev. Lett.* **119**, 181301 (2017) [arXiv:1705.06655 [astro-ph.CO]].
  - [3] D. S. Akerib *et al.* (LUX Collaboration), *Phys. Rev. Lett.* **118**, 251302 (2017) [arXiv:1705.03380 [astro-ph.CO]].
  - [4] A. Pierce, N. R. Shah and S. Vogl, *Phys. Rev. D* **97**, 023008 (2018) [arXiv:1706.01911 [hep-ph]].
  - [5] Y. Bai, H.-C. Cheng, J. Gallicchio, and J. Gu, *JHEP* **1207**, 110 (2012); C. Kilic and B. Tweedie, *JHEP* **1304**, 110 (2013); T. Plehn, M. Spannowsky, and M. Takeuchi, *JHEP* **1208**, 091 (2012); H. Baer *et al.*, *Phys. Rev. D* **96**, 115008 (2017).

- [6] K. Hagiwara and T. Yamada, Phys. Rev. D **91**, 094007 (2015); H. An and L.-T. Wang, Phys. Rev. Lett. **115**, 181602 (2015); S. Macaluso, M. Park, D. Shih, and B. Tweedie, JHEP **1603**, 151 (2016); M. Czakon *et al.*, Phys. Rev. Lett. **113**, 201803 (2014); Z. Han, A. Katz, D. Krohn, and M. Reece, JHEP **1208**, 083 (2012); M. R. Buckley, T. Plehn, and M. J. Ramsey-Musolf, Phys. Rev. D **90**, 014046 (2014); T. Eifert and B. Nachman, Phys. Lett. B **743**, 218 (2015); H.-C. Cheng, C. Gao, L. Li, and N. A. Neill, JHEP **1605**, 036 (2016).
- [7] A. Djouadi and Y. Mambrini, Phys. Rev. D **63**, 115005 (2001); T. Han, K. Hikasa, J. M. Yang, and X. Zhang, Phys. Rev. D **70**, 055001 (2004); M. Muhlleitner and E. Popeno, JHEP **1104**, 095 (2011); M. A. Ajaib, T. Li, and Q. Shafi, Phys. Rev. D **85**, 055021 (2012); M. Drees, M. Hanussek, and J. S. Kim, Phys. Rev. D **86**, 035024 (2012); Z. Yu, X. Bi, Q. Yan, and P. Yin, Phys. Rev. D **87**, 055007 (2013); H. C. Cheng, L. Li and Q. Qin, JHEP **1611**, 181 (2016); M. Abdughani and L. Wu, arXiv:1908.11350 [hep-ph].
- [8] K. Hikasa, J. Li, L. Wu and J. M. Yang, Phys. Rev. D **93**, 035003 (2016) [arXiv:1505.06006 [hep-ph]]; G. H. Duan, K. Hikasa, L. Wu, J. M. Yang and M. Zhang, JHEP **1703**, 091 (2017) [arXiv:1611.05211 [hep-ph]].
- [9] J. Cao *et al.*, JHEP **1211**, 039 (2012); C. Han *et al.*, Eur. Phys. J. C **77**, 93 (2017); C. Han *et al.*, JHEP **1310**, 216 (2013); A. Kobakhidze *et al.*, Phys. Lett. B **755**, 76 (2016); D. Gonçalves, K. Sakurai, and M. Takeuchi, Phys. Rev. D **95**, 015030 (2017); A. Pierce and B. Shakya, JHEP **1806**, 091 (2018).
- [10] M. Abdughani, J. Ren, L. Wu and J. M. Yang, JHEP **1908**, 055 (2019) [arXiv:1807.09088 [hep-ph]]; M. Abdughani, J. Ren, L. Wu, J. M. Yang and J. Zhao, Commun. Theor. Phys. **71**, 955 (2019) [arXiv:1905.06047 [hep-ph]].
- [11] M. Perelstein and A. Weiler, JHEP **0903**, 141 (2009); A. Kobakhidze, N. Liu, L. Wu, J. M. Yang, Phys. Rev. D **92**, 075008 (2015); G. H. Duan, L. Wu, R. Zheng, JHEP **1709**, 037 (2017); N. Liu, *et al.*, arXiv:1910.00749 [hep-ph]; T. P. Tang, L. Wu, H. Zhou, arXiv:1909.02325 [hep-ph]; L. Wu, H. Zhou, Phys. Lett. B **794**, 96 (2019);
- [12] See, e.g., J. Cao, Z. Heng, J. M. Yang, Y. M. Zhang and J. Y. Zhu, JHEP **1203**, 086 (2012) [arXiv:1202.5821 [hep-ph]].
- [13] M. Papucci, J. T. Ruderman and A. Weiler, JHEP **1209**, 035 (2012) [arXiv:1110.6926 [hep-ph]].
- [14] H. Baer, V. Barger, N. Nagata and M. Savoy, Phys. Rev. D **95**, 055012 (2017)

- [arXiv:1611.08511 [hep-ph]].
- [15] K. Griest and D. Seckel, Phys. Rev. D **43**, 3191 (1991).
- [16] A. Djouadi, J. L. Kneur and G. Moultaka, Comput. Phys. Commun. **176**, 426 (2007) [hep-ph/0211331].
- [17] M. Muhlleitner, A. Djouadi and Y. Mambrini, Comput. Phys. Commun. **168**, 46 (2005) [hep-ph/0311167].
- [18] A. Delgado, G. F. Giudice, G. Isidori, M. Pierini and A. Strumia, Eur. Phys. J. C **73**, 2370 (2013) [arXiv:1212.6847 [hep-ph]].
- [19] D. Barducci, G. Belanger, J. Bernon, F. Boudjema, J. Da Silva, S. Kraml, U. Laa and A. Pukhov, Comput. Phys. Commun. **222**, 327 (2018) [arXiv:1606.03834 [hep-ph]].
- [20] G. Aad *et al.* (ATLAS Collaboration), Phys. Lett. B **710**, 49 (2012).
- [21] M. Abdughani, K. Hikasa, L. Wu, J. M. Yang and J. Zhao, JHEP **1911**, 095 (2019) [arXiv:1909.07792 [hep-ph]]; P. Cox, C. Han and T. T. Yanagida, Phys. Rev. D **98**, no. 5, 055015 (2018) [arXiv:1805.02802 [hep-ph]].
- [22] S. Chatrchyan *et al.* (CMS Collaboration), Phys. Lett. B **710**, 26 (2012).
- [23] P. A. R. Ade *et al.* (Planck Collaboration), Astron. Astrophys. **594**, A13 (2016).
- [24] D. Chowdhury, R. M. Godbole, K. A. Mohan and S. K. Vempati, JHEP **1402**, 110 (2014); Erratum: JHEP **1803**, 149 (2018) [arXiv:1310.1932 [hep-ph]].
- [25] M. Aaboud *et al.* (ATLAS Collaboration), JHEP **1801**, 126 (2018) [arXiv:1711.03301 [hep-ex]].
- [26] K. Hikasa and M. Kobayashi, Phys. Rev. D **36**, 724 (1987).
- [27] S. P. Das, A. Datta and M. Guchait, Phys. Rev. D **65**, 095006 (2002) [hep-ph/0112182].
- [28] G. Hiller and Y. Nir, JHEP **0803**, 046 (2008) [arXiv:0802.0916 [hep-ph]].
- [29] C. Boehm, A. Djouadi and Y. Mambrini, Phys. Rev. D **61**, 095006 (2000) [hep-ph/9907428].
- [30] J. Alwall *et al.*, JHEP **1407**, 079 (2014).
- [31] T. Sjostrand, S. Mrenna and P. Z. Skands, JHEP **0605**, 026 (2006).
- [32] J. de Favereau *et al.* (DELPHES 3 Collaboration), JHEP **1402**, 057 (2014).
- [33] M. Cacciari, G. P. Salam and G. Soyez, JHEP **0804**, 063 (2008).
- [34] A. Bartl, W. Majerotto and W. Porod, Z. Phys. C **64**, 499 (1994); Erratum: Z. Phys. C **68**, 518 (1995).
- [35] A. Bartl, H. Eberl, K. Hidaka, S. Kraml, W. Majerotto, W. Porod and Y. Yamada, Phys.

- Lett. B **419**, 243 (1998) [hep-ph/9710286].
- [36] A. Bartl, H. Eberl, K. Hidaka, S. Kraml, W. Majerotto, W. Porod and Y. Yamada, Phys. Rev. D **59**, 115007 (1999) [hep-ph/9806299].
- [37] D. Ghosh, Phys. Rev. D **88**, 115013 (2013) [arXiv:1308.0320 [hep-ph]].
- [38] Z. Kang, J. Li and M. Zhang, Eur. Phys. J. C **77**, 371 (2017) [arXiv:1703.08911 [hep-ph]].
- [39] H. An, J. Gu and L. T. Wang, JHEP **1704**, 084 (2017) [arXiv:1611.09868 [hep-ph]].